PCCP

Accepted Manuscript

Nucleic acid ion structures in the gas phase

Josephine Abi-Ghanem,[1,2,3] Valérie Gabelica[*,2,3]

[1] CNRS, UMS 3033, IECB, F-33600 Pessac, France

[2] Univ. Bordeaux, IECB, ARNA laboratory, F-33600 Pessac, France

[3] INSERM, U869, ARNA laboratory, F-33000 Bordeaux, France

* Corresponding author: valerie.gabelica@inserm.fr

Abstract

Nucleic acids are diverse polymeric macromolecules that are essential for all life forms. These biomolecules possess functional three-dimensional structure under aqueous physiological conditions. Mass spectrometry-based approaches have on the other hand opened the possibility to gain structural information on nucleic acids from gas-phase measurements. To correlate gas-phase structural probing results to solution structures, it is therefore important to grasp the extent to which nucleic acid structures are preserved, or altered, when transferred from the solution to a fully anhydrous environment. We will review here experimental and theoretical approaches available to characterize the structure of nucleic acids in the gas phase (with a focus on oligonucleotides and higher-order structures), and will summarize the structural features of nucleic acids that can be preserved in the gas phase on the experiment time scale.

I. Introduction

Nucleic acids (NA) are polymeric macromolecules that are essential molecules of life. They are involved in the storage, transmission and processing of cellular information. NAs are made from monomers called the nucleotides, and include the deoxyribonucleic acid (DNA), and the ribonucleic acid (RNA) (Figure 1). To determine the three-dimensional (3D) structure of NAs and other macromolecules at atomic resolution, the classical approaches are X-ray crystallography[1] and nuclear magnetic resonance (NMR).[2, 3] However, despite technological advances in the instrumentation and sample preparations in the past years, both methodologies still present some stringent limitations concerning the amount and purity needed, and molecular

properties such as solubility, flexibility, and polymorphism, which can sometimes hamper structure determination.
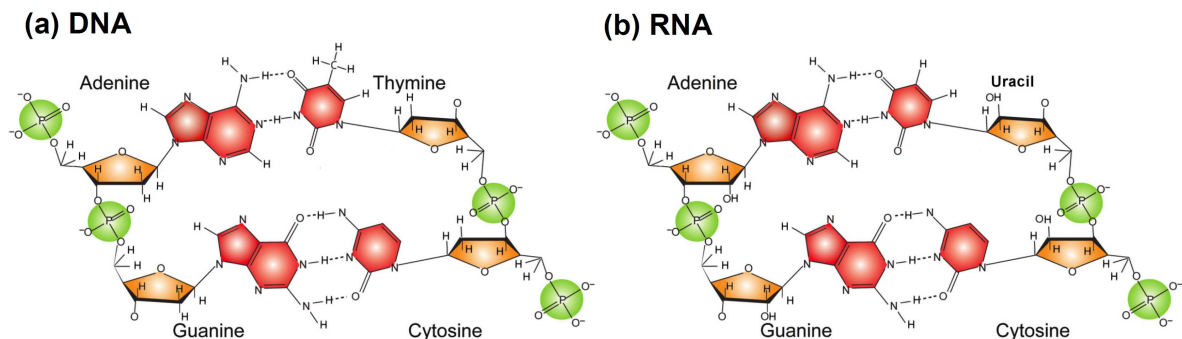

Figure 1: DNA and RNA bases and their interaction in a double helix.

For this reason, alternative approaches were sought to complement these high resolution methods. Although they provide low resolution information on a structural point of view, techniques such as circular dichroism (CD)[4], small angle X-ray scattering (SAXS)[5] provide complementary information to assist 3D structure representation. Mass spectrometry (MS) is a highly versatile technique in many areas of science and technology. The particular strengths of mass spectrometry are the rapidity of data acquisition, the low sample amount requirements, and the possibility to separate complex mixtures. Moreover, as the detection is mass-based, there is no requirement for molecule modification, labelling (in contrast with fluorescence techniques) or immobilization (in contrast with single-molecule force spectroscopy or with surface plasmon resonance). Mass spectrometry is therefore able to provide information on flexible or disordered molecules to which X-ray crystallography and NMR methods are blind.[6]

However, in contrast with the other methodologies, MS records all information in the gas phase. The appearance of soft ionization techniques, namely electrospray ionization (ESI) and matrix-assisted laser desorption/ionization (MALDI) has enabled one to transfer large macromolecules ranging from nucleosides and oligonucleotides till intact ribosomal assemblies into the gas phase [7]. Large individual NAs were studied by ESI like the lambda phage DNA of a molecular weight of $31.5 * 10^6$ Da an the Coliphage T4 with a molecular weight of 10^8 Da. [8, 9] The MS experiments are of high interest because they present the possibility to separate and

characterize each component present in a complex mixture. Several methods for structural probing with MS, with particular focus on probing after the transfer from the solution to the gas phase, will be reviewed here.

The literature on structural probing in the gas phase can be divided in two categories: (1) studies of the gas phase structure *per se*, taking advantage of the vacuum environment to study the intrinsic properties of biomolecules in well-defined energetic conditions, and (2) studies of the gas phase structure with the aim to trace back information on the initial structure the molecules had in the starting solution. However, structural probing occurs in the gas phase, and while the gas-phase structure and energetics are fundamentally interesting, these methods will truly become of interest to the biologist only if the solution-phase structure is preserved in the gas phase. Therefore, for the latter type of applications, the gas-phase structural ensemble should preferably be a metastable state, kinetically trapped in a local minimum which is close to the initial solution-phase structural ensemble, rather than the energetically most stable state in the gas phase. We will therefore not only discuss differences in the most stable states in solution vs. *in vacuo*, but also consider the kinetics of conformational changes from the solution structure to the vacuum structure, the energy barriers that can be overcome or not for certain rearrangements, and the time scale of the gas-phase experiments.

The importance of the solvent and counter-ions was already noted in the formation of the 3D structure of NAs.[10] While the structure of NA is well known in solution, it is unclear how they react when transferred to a fully anhydrous environment, and how fast they do so. Intuitively one can think that, when the molecule or complex is transferred to gas phase during the evaporation, it would lose key non-covalent interactions responsible for its secondary, tertiary and quaternary structure, and this raises many questions with regard the extent of structural change upon vaporization, and the possibility to infer solution structure from gas phase measurements. However, as described below, experimental approaches show that, even in the gas phase, proteins [11] and nucleic acids tend to retain their overall structure, and most inter- and intra-molecular interactions are preserved if using mild desolvation. This is clearly revealed by the observation of intact non-covalent complexes (quaternary structures) of proteins[12], protein complexes with small ligands[13], and nucleic acid[14] in the gas phase. In terms of shape preservation, biomolecules produced by electrospray ionization from native solution adopt relatively low charge states and a compact form that may retain a memory of their solution state. We will review here the current knowledge of the structure of NA from the secondary to the quaternary structure, and the experimental and theoretical approaches available to grasp the structure of NA in the gas phase as

3

studied in mass spectrometry conditions. More detailed discussions of each topic, as well as applications to biological problems, can be found in a recent book.[15]

II. Transferring nucleic acids from the solution to the vacuum

The most widely used experimental approach to transfer intact biomolecule structures from solution to gas phase is electrospray (ESI)[16]. In general, the transfer into the gas phase of nucleic acids is mainly performed in the negative mode, generating deprotonated NAs. This is both for sensitivity reasons, and for keeping the same net charge as in solution for native mass spectrometry.[17] However, there's a possibility to observe NAs in the positive mode either through the cationisation with monovalent cations (Na^+) or by protonation.[18, 19] The solution containing the NA is introduced into a capillary on which a negative potential is applied compared to the counter-electrode that is the entrance of the mass spectrometer, and the naturally negatively charged NA will be preferentially enriched in the negatively charged droplets formed at the tip of the capillary under the influence of the electric field. The NA molecules bear their negative charge on the phosphates. Usually, not each and every phosphate is deprotonated: most are neutralized by protons coming from the solvent or from ammonium ions present in solution (ammonium acetate is a typical buffer for nucleic acids analysis by ESI). Small oligonucleotides (1 to 5 nucleotides) can be detected as singly charged ions $[NA-H]^-$ (NA representing the neutral nucleic acid with phosphate groups fully neutralized by protons), but multiply deprotonated ions $[NA-zH]^{z-}$ can be observed as soon as at least two phosphate groups are present. For each oligonucleotide, this usually results in a charge state distribution (a distribution of probabilities to accommodate a given total amount of negative charges as deprotonated phosphates). Ions produced by ESI are closed-shell ions.

The high electric field on the tip of the capillary generates a spray of highly charged droplets (containing the NA, the solvent, and buffer) which will travel down potential and pressure gradients towards the inside of the mass spectrometer. As the droplets move towards the mass spectrometer, the solvent will evaporate and the charge density will increase. At a critical point called the Rayleigh limit, charged droplet instability will result in their asymmetric Coulomb fission, generating smaller droplets which carry away excess charges (among which, nucleic acid polyanions) from the surface of the parent droplet[20] (Figure 2). When starting from dilute solutions, it takes only a few of these asymmetric fission steps, occurring presumably on the

4

microsecond time scale, to end up with a nanodroplet containing an isolated nucleic acid surrounded by solvent and some counter-ions. The last steps of solvent evaporation from the NA are assumed to occur following the "charge residue mechanism" (CRM).[21, 22] The CRM states that the solvent and volatile buffer molecules progressively evaporate from the droplet containing only one analyte until the fully desolvated and declustered charged analyte remains.[11] The chain ejection mechanism (CEM) recently suggested for unfolded proteins[23] is not very likely to apply to nucleic acid chains, because their degree of hydrophobicity/hydrophilicity is homogeneous throughout the chain. Final evaporation of solvent and counter-ions (if volatile) from the droplets will lead to the fully dehydrated nucleic acids observed in the mass analyser.
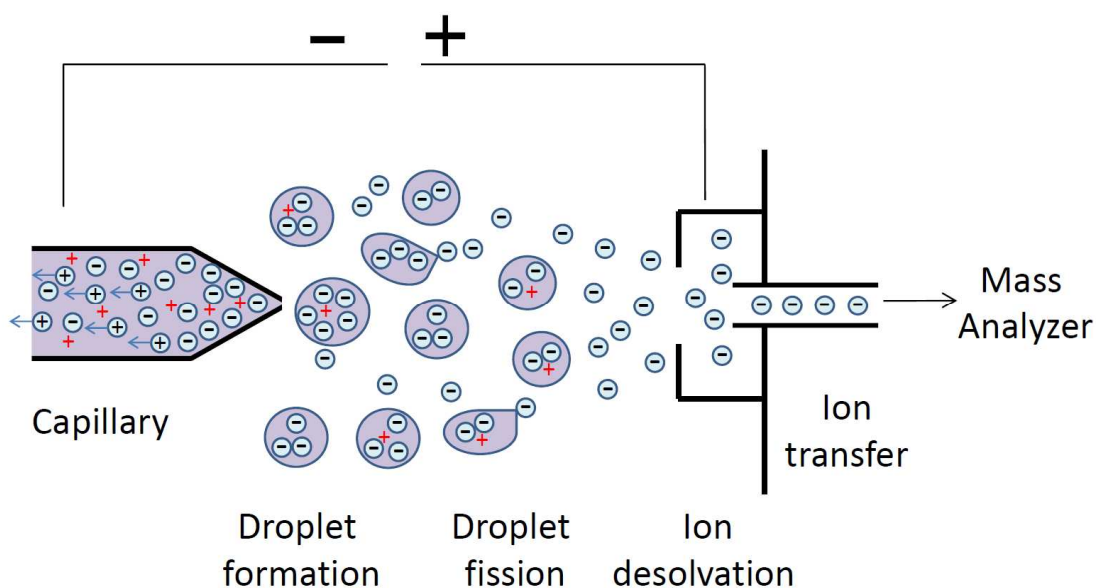
Figure 2: Schematic of the successive steps of the electrospray process (shown here in the negative ion mode). The liquid sample is injected through a capillary on which a negative voltage is applied, and negatively charged droplets are formed (excess of negative ions shown in blue compared to positive counterions, e.g., Na^+ or NH_4^+, shown in red).

The typical mass spectrum of a 14-mer double-stranded DNA is shown in Figure 3. Here the two single strands differ in mass, and are detected in the 3- charge state. The duplex is detected predominantly in the 6- and the 5- charge states. The duplex peaks are observed at m/z

$$m/z = [MW_{(ss1)} + MW_{(ss2)} - z*1] / z$$

Where $MW_{(x)}$ are the molecular weights of the neutral constituent strands (ss1 and ss2), z is the charge state, and 1 is the mass of a proton.

The peaks causing a tail on the right hand side of the fully deprotonated species are due to the replacement of some of the protons of the phosphates by sodium cations (which are not volatile, i.e. they cannot be eliminated by increasing the internal energy of the system) or for ammonium cations (which are volatile, i.e. they can be eliminated as neutral ammonia by increasing the internal energy of the system).
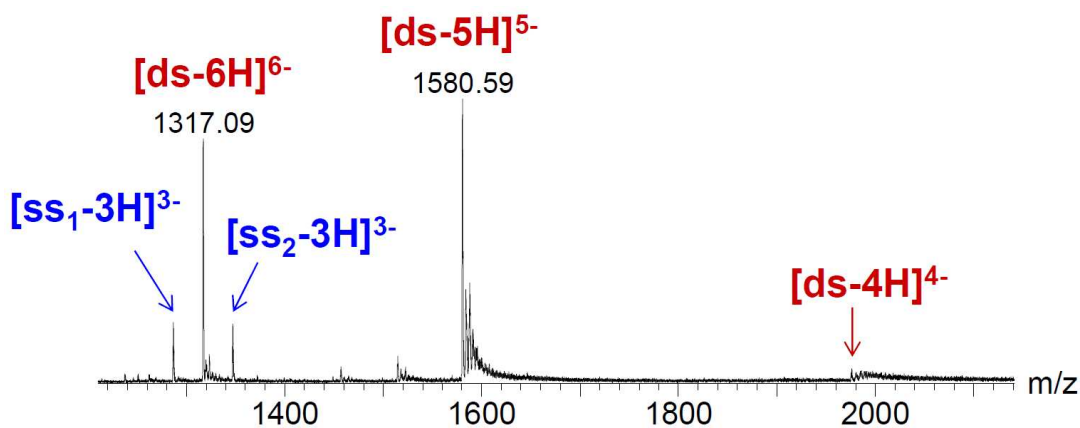

Figure 3: Typical ESI mass spectrum of a 14-mer double-stranded DNA (noted "ds") constituted from the perfectly complementary single strands "ss_1" (5'-GGGGTCGTAGTGGC-3') and "ss_2" (5'-GCCACTACGACCCC-3'), mixed at 5 μM in 100 mM NH_4OAc.

The internal energy of the charged ions is therefore very important and influences the aspect of the mass spectra. At high internal energy, ions fragment faster (or, at fixed reaction time window, fragment to a greater extent) whereas with low internal energy, little fragmentation occurs.[24, 25] It is important to stress out that instrumental conditions that favour low internal energies are usually those that lead to preserved structures, but not usually those that lead to the sharpest mass spectra. There is always a trade-off between desolvation and volatile buffer evaporation on the one hand, and rupture of noncovalent intra- and inter-molecular interactions on the other hand.

In general, ESI produces ions with lower internal energy than MALDI, and therefore allows the study of intact biomolecules or non-covalent complexes. However, the internal energy of the ions depends not only on the ionization method, but also on all thermal and collisional heating that could occur inside the instrument, and therefore the tuning of the pressures and the accelerating voltage needs to be optimized to complete ion desolvation while preserving weaker interactions. Therefore the control of the internal energy is essential for the study of NA structures

in the gas phase. One way to define the ion internal energy is through the effective temperature (the temperature of the Boltzmann internal energy distribution of the ion population that would give the same effect as observed experimentally).[24, 25] However, assessing the effective temperature of ions inside the droplets, during the final stages of droplet evaporation, and during ion transit in the zones of the mass spectrometer where they can undergo collisional activation or collisional cooling is far from trivial. The thermodynamics aspects of the vaporization process are not well understood, but they should involve a balance between collisional heating to enable evaporation and endothermic cooling upon evaporation.[26-28] Therefore the comparison between experimental and theoretical results are not necessarily straightforward.[11]

III. MS-based approaches providing structural information on nucleic acids and their complexes

III.1. In-solution labelling followed by MS detection

Information about the higher order NA structure in solution can be obtained by chemical or isotopic probing of NA molecules in solution before transferring into the gas phase for mass spectrometry detection. The general workflow is shown in Figure 4. Nucleotide specific labelling reagents include dimethyl sulfate (DMS), 1-cyclohexyl-3-(2-morpholinoethyl)-carbodiimide metho-*p*-toluene sulfonate (CMCT), and β-ethoxy-α-ketobutyraldehyde (kethoxal, KT). The different probes provide unique mass signatures, which can be resolved readily and unambiguously by mass analysis. MS had helped in the elucidation of many modified ribonucleotides[29, 30] as well as modified DNA[31]. For RNA, a strategy called MS3D emerged from the combination of MS detection with structural probing [32]. This MS-based footprinting technique takes advantage from the 3D assembly of NA: the Watson-Crick base pairing rules that usually define the higher order structure of NA is complemented by information on the detection of labelled sites for each nucleobases, thereby leading to more comprehensive information on base pairing in the NA structure. The structure of the putative feline immunodeficiency virus (FIV) ribosomal frame shifting pseudoknot (PK) has been investigated by MS3D approach, which involves the application of established solvent-accessibility probes and chemical crosslinkers with detection by electrospray ionization (ESI) Fourier transform mass spectrometry (FTMS).[33]
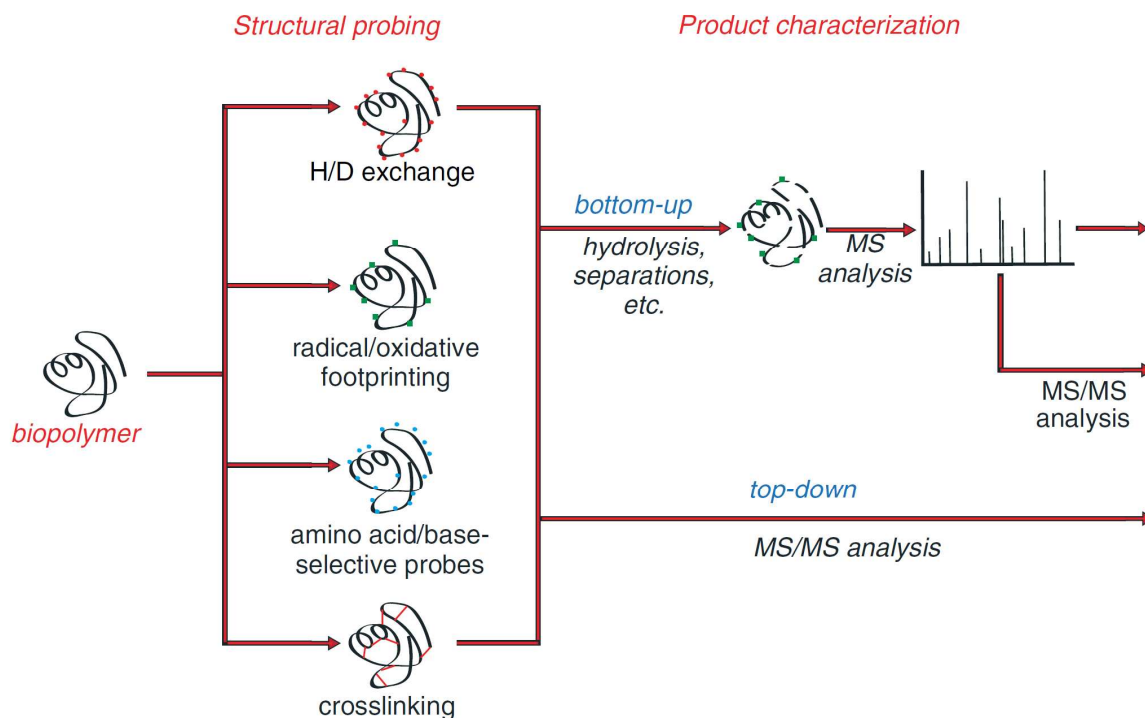
Figure 4: General strategies for nucleic acid structural probing by in-solution labeling followed by MS detection. The substrate of interest (biopolymer) is treated with the selected labeling agent (deuterated solvent for H/D exchange, OH• radicals for oxidative footprinting, covalent label for base-selective probing, bidentate agents for crosslinking). The products can undergo purification/enrichment procedures, or can be analyzed directly by mass spectrometry, according to bottom-up or top-down strategies (figure reprinted from Fabris and Yu, J. Mass Spectrom (2010), with permission from John Wiley & Sons, Ltd.).[32]

III.2. Tandem mass spectrometry (MS/MS)

III.2.1. MS/MS to localize labelled sites

Tandem mass spectrometry is a MS methodology involving at least two stages of MS with fragmentation occurring in-between (Figure 5a). In this approach, the NA is introduced into the mass spectrometer as an ion, the ions of a given m/z ratio are selected, then an external stimulus such as collisions, photon absorption, or electron interaction will induce some fragmentation of the parent ion by cleaving the covalent bond to produce the product ion which will be then assessed by MS. Up to now, only collision-induced dissociation (CID) MS/MS was used to investigate chemically labelled sites, and the potential of emergent techniques such as electron detachment dissociation (EDD),[34] electron transfer dissociation on negative ions (nETD),[35] or electron photodetachment dissociation (EPD)[36] remains to be evaluated. Gas-phase fragmentation

of nucleic acids can be generally used in the areas of sequencing, identification of single nucleotide polymorphisms (SNP) [37], identification and location of modified bases [38, 39] etc… The MS/MS method is also used to localize the sites of chemical probing because the fragmentation will not affect the labelling site.[40, 41] MS/MS can also be used to probe the structure in gas phase and the identification of the nucleotides making direct contact with the ligand and the mapping of the location of the corresponding motif.[42, 43] This gas-phase footprinting technique successfully localized sites on different stem-loop domains of the HIV-1 packaging signal, correlating their location with the position of known contacts between these structures and the viral nucleocapsid protein.[44, 45] The integration of chemical labelling methods with MS/MS has become also an increasingly popular strategy for structural biology studies.

III.2.2. MS/MS for direct gas-phase structural probing by slow heating methods

Collision-induced dissociation (CID) is the most widespread fragmentation method because it is widely available on commercial mass spectrometers equipped for tandem mass spectrometry (MS/MS).[46] The principle is to increase the internal energy of the ions and to observe the resulting fragments. It has been suggested that the base pairing of a double helix can have a masking effect from the fragmentation, and therefore protecting higher order structures and to observe preferentially the fragmentation of unpaired bases.[47, 48] When fragments result from non-covalent bond cleavage, it also is possible to infer how the observed fragments and rates are correlated to the reactant's structure. For example, by comparing the kinetic stability of duplexes with varying sequences, it was concluded that hydrogen bonding and base stacking were preserved in the gas phase.[49, 50] The main caveat of this reasoning is the speculative aspects of MS/MS interpretation: the observable depends not only on the reactant structure, but also on the reaction pathways leading to the transition state. In the slow heating conditions of CID, significant rearrangements can occur before the fragmentation takes place, especially for large complexes. To probe gas-phase structures that have maximal chances to have remained similar to those that were present in solution, it is preferable to avoid fragmentation methods.

Blackbody infrared radiation-induced dissociation (BIRD)[51] has been used to provide quantitative measurements of gas-phase dissociation activation energies and entropies for DNA duplexes. In BIRD, the ICR trap mass spectrometer cell walls are heated, and IR photons emitted by blackbody radiation from the cell walls are absorbed by the ion. When photon abosorption and re-emission is fast compared to dissociation, the ion internal energy distribution is a Boltzmann distribution, and Arrhenius parameters E_a and A can be extracted from temperature-dependent kinetic experiments. E_a and A can be interpreted in terms of ion structure and energetics.[52]
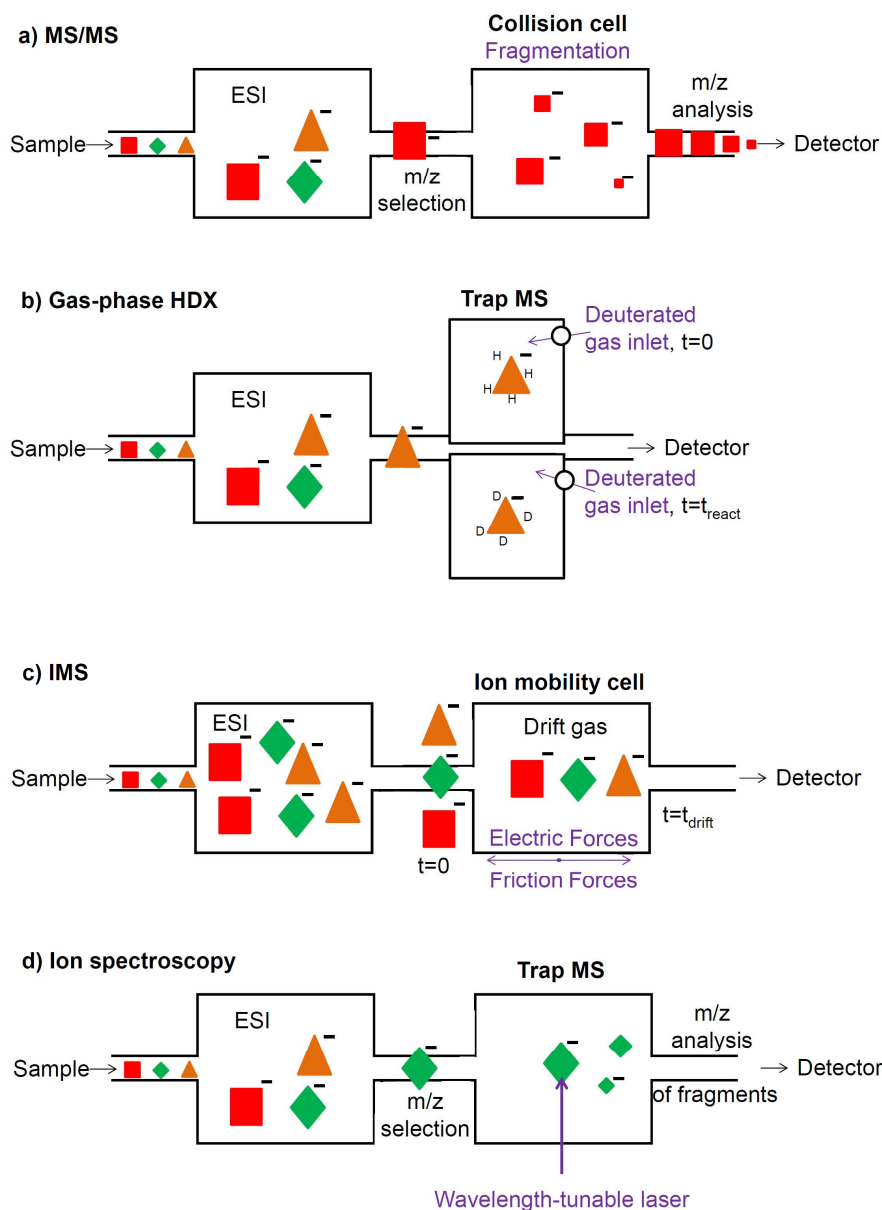
Figure 5: Schematic representation of some MS-based gas-phase structural probing approaches: (a) Tandem mass spectrometry (MS/MS; see paragraph III.2), the sample is infused, ionized, and precursor ions are selected based on their m/z. The product ions formed in the collision cell are then mass analysed. (b) Gas phase hydrogen/deuterium exchange (HDX; see paragraph III.3). In a trap-type mass analyser, deuterated gas will be injected and ions are allowed to react during a certain period of time, during which hydrogen will be exchanged for deuterium. Mass spectra are recorded at different reaction time intervals. (c) Ion mobility spectrometry (IMS; see paragraph III.4). Ions are bunched and sent into an ion mobility cell. In a drift tube IMS, ions are separated in time based on the steady state velocity achieved when the acceleration due to the electric field is compensated by friction with a gas. (d) Ion spectroscopy (see paragraph III.5). The sample is injected and ionized. In the ion trap, ions of selected m/z are subjected to photon irradiation, which causes fragmentation. The product ion spectra are recorded as a function of the irradiation wavelength to reconstruct the ion's optical spectra.

William's group studied by BIRD the dissociation kinetics of a series of complementary and non-complementary DNA duplexes, $(TGCA)_2^{3-}$, $(CCGG)_2^{3-}$, $(AATTAAT)_2^{3-}$, $(CCGGCCG)_2^{3-}$, $A_7 \cdot T_7^{3-}$, $A_7 \cdot A_7^{3-}$, $T_7 \cdot T_7^{3-}$, and $A_7 \cdot C_7^{3-}$ and concluded that Watson-Crick base pairing that exists in solution is preserved in the gas phase. [49] Daneshfar et al. studied the thermal decomposition of a series of T-rich doubly deprotonated oligodeoxynucleotides of 10-, 15- and 20-mer were Arrhenius activation parameters for the loss of neutral nucleobase have been determined. The authors found that the loss of a nucleobases is sensitive to its identity and location in the oligodeoxynucleotide, and found a trend in the values of E_a: A<G<C. They pointed that the differences observed in E_a comes not only from the bases identity but also from the ability of the nucleobases to participate in intramolecular interactions. [53, 54] Infrared multiple photon dissociation (IRMPD) can also be used in a similar way to BIRD, provided that slow heating conditions (slower dissociation rates than photon absorption/emission rates) are maintained.[55] IRMPD was recently applied to megadalton-sized DNA; note however the dissociation rates were quite fast.[56] At high laser power, the onset times of fragmentation are short (typically a few milliseconds), and it is possible that dissociation of excited ions competes with photon absorption or emission, with ion dissociation no longer in the so-called rapid exchange limit (REX), for which the internal energy distribution of excited ions follows a Boltzmann distribution at any time. [57]

III.3. Gas-phase labelling using ion-molecule reactions inside the mass spectrometer

Here the nucleic acid ion reactivity with molecules (or sometimes with other ions) is monitored directly in the gas phase: the mass spectrometer serves both as the reactor and the detector. The best known technique is gas-phase hydrogen/deuterium exchange (HDX) (Figure 5b). The charged biomolecule of interest is stored in a trap-type mass spectrometer for different periods of time, while leaking in volatile deuterating reagents, such as D_2O, CH_3OD or ND_3. By recording the mass spectrum as a function of storage time, this allows a study of the gas phase HDX kinetics. Because exchangeable hydrogens buried inside the biomolecule are expected to exchange very slowly compared to those exposed on the surface, the H/D-exchange kinetic data should contain information on the three-dimensional structure. The HDX can be also coupled to ion mobility spectrometry[58] or to a fragmentation methodology like electron transfer dissociation (ETD)[59] to assess a higher resolution for the biomolecule structure. Mo et al. showed that gas-phase HDX may be used to characterize nucleic acid higher order structure. Their results on the

stability of different nucleic acid hairpins in gas phase HDX experiments show a correlation with those in solution.[60] However, the *de novo* interpretation of reaction rates in the gas phase in terms of structure is extremely challenging already for dinucleotides[61, 62], and virtually impossible for nucleic acids of biologically relevant size. For example, G-quadruplexes undergo much faster HDX than single strands[63], but that is counterintuitive given that guanines should be protected by being engaged in G-quartets, and totally different from the behaviour in solution.

III.4. Ion mobility spectrometry (IMS)

Ion mobility spectrometry (IMS) is based on the separation of ions according to their drift velocity in an inert bath gas at high pressure, under the influence of an electric field (Figure 5c). The ion's mobility gives information on the ion's size and shape via the momentum transfer collision cross section (CCS_{exp}, in $Å^2$).[64, 65] In other words, CCS_{exp} indicates the extent to which the ion is slowed down by the gas and the shape of the molecule. Collision cross section is related to the size and overall fold of macromolecules structure.[66] The challenge however lies in how to achieve the structural assignment from CCS_{exp}. This means that structural details need to be added from theoretical approaches (see section IV), which in turn need to be validated by their ability to reproduce available low-resolution experimental information.

The IMS data interpretation in terms of structure is closely linked to simulation *in vacuo* which try to cluster the structures by calculating their collision cross sections CCS_{calc}, and to match them with CCS_{exp}. This approach consists in simulating the NA in gas phase (molecular dynamics (MD) simulation for oligonucleotides, *ab initio* or density functional theory (DFT) calculation for up to dinucleotides only), then calculating a CCS_{calc} for each structure extracted from those calculations. Many points of this protocol are to date still questionable or need improvement. The structural simulations are discussed in Section IV below. Regarding the calculation of CCS_{calc}, several methods exist. The most common models used to calculate CCS_{calc} are the projection approximation (PA)[67], the exact hard-sphere scattering (EHSS)[68] and the trajectory method (TM)[69], all of which were parameterized to determine the CCS in helium buffer gas. An optimisation of the original EHSS algorithm was developed (EHSSrot) to lower the computational cost by reducing the number of ion rotation steps through evaluation of multiple ion/buffer collisions per orientation.[70] Besides, Siu *et al.* optimized the atomic collision radii based on DFT calculations for EHSS calculations on peptides[71], and our preliminary results show that these optimized EHSS parameters work reasonably well for nucleic acids too. Recently a new

approach called the projection superposition approximation (PSA) was introduced.[72-75] The method is similar to the PA concept, but soft spheres account for the additive contribution of several atoms, and a shape factor accounts for the molecule's concavity. Larriba and Hogan proposed another model using all-atom models of particles and non-specular, inelastic gas-molecule scattering from particle surfaces.[76] The last two methods were conceived in order to account for CCS both in He and N_2 drift gasses. Indeed, it is important to note that the CCS values measured in He or N_2 differ due to the intrinsic size difference of the two buffers, and that most commercial instruments are operated in nitrogen. Therefore the comparison between CCS_s in N_2 and He is not straightforward and was shown to depend on the class of molecules.[77] So far the correlation has not been explored for nucleic acids.

In conclusion, although the structural information extracted from ion mobility spectrometry is relatively limited, the IMS coupled to molecular dynamic *in vacuo* remains very promising to obtain information on gas-phase structure, but this will require addressing fundamental questions in collision cross section interpretation. Also, although it becomes more and more widespread thanks to the availability of commercial instruments, ion mobility spectrometry remains inherently a low resolution structural characterization method, and there is an evident need for complementary approaches that can reveal secondary and tertiary structures in more detail.

III.5. Ion spectroscopy

Ion spectroscopy is based on the same principles as traditional solution spectroscopy (Figure 5d). The main difference is that, due to the low ion density in the gas phase, absorption cannot be measured by attenuation of the beam light. Ion spectroscopy is instead an *action* spectroscopy: resonant interaction with a photon is detected by monitoring the action of photons on ions (usually fragmentation) as a function of the wavelength. A molecule in the gas phase is free to rotate relative to a set of mutually orthogonal axes of fixed orientation in space, centred on the center of mass of the molecule. Microwave spectroscopy coupled to highest-level calculations provides the highest resolution structural data but can be applied to small molecules only, such as isolated nucleic acid bases.[78-82]

The most widespread approach is infrared (IR) ion spectroscopy, which is the ideal method to probe hydrogen bonding in the gas phase. The dissociation requires the resonant

absorption of multiple IR photons, and therefore the method is named IRMPD (infrared resonant multiple photon dissociation) ion spectroscopy. The structural interpretation of experimental data is based on the matching between the experimental and the theoretical IR spectra expected for a proposed gas-phase structure. This approach works well for small ions like mono- or dinucleotides.[83, 84] Salpin et al. first studied protonated nucleotides (uracil, cytosine and thymine) by IRMPD.[83] This study shows that the lowest energy tautomer for these pyrimidines is the enol form, and the second most stable the oxo tautomer was present; however it was observed with a very small signal. Further analysis on the tautomerism of the cytosine and uracil by IR spectroscopy showed that the two protonated forms are formed and originate from the electrospray conditions.[85, 86] The same results were obtained using electronic absorption spectroscopy experiments. [87-89]

A recent IRMPD spectroscopy study on dimers of cytosines and modified cytosines showed the presence of the alignment of nucleobases analogous to that of the DNA *i*-motif.[90] Deprotonated nucleotide were investigated by Nei et al., which showed by IRMPD and theoretical calculations that in NA the most stable conformation of adenine, uracile/thymine and cytosine is when the ribose is in C3' endo and the base in an anti conformation while a guanine have a C3' endo sugar but a syn conformation for the base.[91, 92] With regard to larger nucleic acid structures, Gabelica *et al.* explored IR multiple-photon dissociation spectroscopy for G-quadruplex models of biologically relevant size (24 bases)[93], and of zwitterionic i-motif structures[94], but although band shifts confirm hydrogen bond formation by the bases in the gas phase, the spectra were too cluttered to extract other structural information.

One way to obtain higher resolution IR spectra is by IR-UV double resonance spectroscopy on cold species. Many such studies were performed on neutral nucleic acid building blocks in order to establish the intrinsic properties of individual DNA and address the structural properties of the base pairings in NAs (for a review, see [95]). The first resonance-enhanced multiphoton ionization (REMPI) investigation concerned a GC base pair and studied the spectroscopic characterization of the hydrogen bonding in isolated guanine-cytosine: It was found that the gas-phase GC base pair adopts a single configuration, which may be Watson-Crick. [96] The vibronic spectrum of the adenine-thymine (AT) base pair was obtained by one-color resonant two-photon ionization (R2PI) spectroscopy, and in contrast to the GC base pair, the Watson-Crick AT base pair is not the most stable isolated and its vibrational spectrum is not in agreement with the observed experimental spectrum.[97] More recently, cold ion spectroscopy was carried out on cationized and protonated nucleic bases and base pairs.[88, 89] The gap between nucleotides and

large NAs however, has not yet been bridged in the way it has been for peptides by Boyarkin and Rizzo.[98, 99]

Electronic spectroscopy alone has also the potential to provide structural information in the gas phase, as the chromophore absorption or relaxation pathways may depend on its surrounding by other chemical groups. Interestingly, the absorption wavelength of isolated bases, as measured by action spectroscopy (fragmentation) in the gas phase is not very much shifted compared to the absorption in aqueous solution.[100, 101] In the case of larger nucleic acids, the main action following irradiation of DNA multiply charged anions by UV light is the resonant ejection of an electron.[36] This provides an efficient way to perform action UV spectroscopy. Recently, UV-induced electron photodetachment were exploited to perform electronic (UV) ion spectroscopy of single strand, duplex, and G-quadruplex structures, but similarly to what happens in solution, UV band shifts upon structuration and base stacking are only very subtle.[102] These, and other isolated attempts to probe nucleic acid structure by fluorescence[103, 104] or photoelectron spectroscopy (PES)[105, 106] are currently purely exploratory. The gas phase structures are very sensitive to the location of the charges on the molecules. To assess the correct structure, one must be able to localize the exact position of the charges and so are spectral properties. PES could be a potential method to probe the localization of the charges around the molecule by probing the corresponding repulsive electrostatic interactions on the charged molecules. Although promising in terms of structure discrimination, each new gas phase method requires deeper fundamental investigation to obtain rules that can relate the observable to structural features.

IV. Simulation of nucleic acid structures in gas phase

The structural information obtained from the MS methodologies mentioned above are often coupled to computational approaches in order to unravel the atomistic details of the nucleic acids while being transferred from solution towards gas phase, and to study their gas-phase stability (or metastability). We will describe below an overview of the theoretical calculations in gas phase nucleic acid ions, and the associated challenges.

IV.1. Charge location

On small singly deprotonated nucleotides, ion spectroscopy experiments combined with DFT calculations have shown that the negative charge is located on the phosphates.[91, 92] For multiply charged ions, although we know for each *m/z* peak the total integer number of charges on

the whole molecule, the distribution of the charge sites along the molecule is a major source of uncertainty. For longer nucleic acids, the negatively charged phosphates are likely to be the strongest base accessible to proton capture for the partial neutralization (see Section II above). Hoaglund *et al.* were the first to show using IMS that the gas-phase conformation depends strongly on the total number of charges on a single stranded dT_{10}.[107] Later, MD simulations with two different setups on a double helix was performed for distributing the charge along the backbone of the NA.[108] One is considering that every phosphate is charged and basically the net charge is distributed evenly on all the phosphates. Another way is to localize the phosphate group which have a net charge of -1 and to protonate the rest of the phosphate group. The authors concluded that both methodologies used on a DNA double helix do not give significantly different results in terms of structure.[108] In conclusion, while testing different specific charge locations remains feasible on small systems, the delocalized charge model is preferred for larger systems for sake of simplicity.

IV.2. Computational approaches

Quantum-chemical methods such as the density functional theory (DFT) are powerful computational method to assess the structure of DNA[109-111] and RNA[112-115] mononucleotides in the gas phase. However, because the ESI permits the evaporation of the intact molecule with a range of internal energies corresponding to an effective temperature at or above room temperature, multiple low-energy conformers are accessed in the experiments rather than only the most stable conformer. Recently a global study by Nei et al. showed the gas phase structures of the four deprotonated mononucleotides by comparing the measured IRMPD spectra with the linear IR spectra calculated at the B3LYP/6-311+G(d,p) of DNA and RNA.[91, 92] This level of theory allowed the identification of the conformations present in the experiments. However, the DFT methodology is limited to small molecules for its time consuming calculations.

A theoretical study using time-dependent DFT (TDDFT) was used to compute the electronic transitions of the nucleic acid bases (guanine, adenine, cytosine, uracil and thymine). The authors found a good agreement between the computed energies and the corresponding experimental data. [116] Recently, TDDFT calculations were used in order to study more complex systems as in the parallel and anti-parallel G-quadruplexes. The calculations reproduced qualitatively the experimental absorption and ECD spectra obtained and identified the responsible structures of the excited stated for the two types of G-quadruplexes. [117] On the quantitative point of view, however, the applied scaling factor highlights that progress is still needed to assign electronic spectra of multi-base systems and interpret them in terms of structure.

Larger nucleic acids are being simulated in the gas phase by molecular dynamics, although force fields are usually developed for simulating biomolecules in aqueous solution. Nevertheless, the recent force fields such as Parmbsc0, adapted to nucleic acids[118], can be used to study the structure in gas phase, and this makes sense given that some parameters are derived from *ab initio* calculations *in vacuo*. MD simulations are done assuming a constant energy or constant temperature ensemble. We have however seen above that an ion in the gas phase is not at equilibrium with its surroundings (the ion population is a microcanonical ensemble) and that the effective temperature in the experimental setup is an inherently difficult parameter to determine. Also, the time step of the MD should also be reduced in the gas phase compared to solution simulations because the motions of the biomolecules are not dampened by surrounding solvent. There are therefore several non-trivial, challenging aspects in defining the input MD simulation conditions when the objective is to compare with real experimental conditions (temperature, pressure, and time scale).

IV.3. In vacuo structure compared to solution structures

The gas-phase MD simulations are started by placing a solution-phase equilibrated structure in the gas phase. A fundamental question is whether the theoretical calculations of the three-dimensional structures in gas phase are equivalent to (or at least, keep a memory of) the structure in solution. Some research already addressed this question in the proteins field.[119,11] A proteome-scale study suggested that the structure in gas phase is in general very close to the one in solution. The authors showed that the structure in the gas phase maintains its structural features compared to the solvated molecule[120]. In contrast with proteins,[11] NAs usually have a non-globular conformation and can present some structural perturbations due to their flexibility, so one must be careful not to blindly extrapolate results from the protein field. Nevertheless, the preliminary results so far in the nucleic acids field are encouraging (see below), as many experimental and theoretical studies established that the representation of NA in gas phase structurally resembles to the one in solution phase. In the next section we will discuss these results, classified by type of NA structure.

V. Nucleic acid structure in the gas phase: experimental and theoretical results

V.1. Single strand DNA

Single stranded DNA has been studied in the gas phase experimentally first using oligothymidine comprising ten thymines by ESI and IMS methodology.[107] The obtained CCS_{exp} and CCS_{calc} with different type of charges and localization of charges along the oligonucleotide showed that when charges reside at adjacent sites, the conformer is essentially linear over the deprotonated region and globular over the remaining portion. Gidden *et al.* studied by IMS and molecular modelling (series of simulated annealing and energy minimization) the conformation of dinucleotides. They showed that even with its relatively simple systems, the dinucleotides showed a complex conformational and energetic properties (up to three conformations were identified for some of the dinucleotides) (Figure 6).[121] A study on trinucleotides showed a more stable conformation, and IMS coupled to MD was used to study the possibility of the zwitterion formation.[122] Investigations of the conformations of deprotonated trinucleotides (dTGT, dGTT and dTTG) showed that dTGT is not a stable zwitterion in the gas phase. IMS was also applied to study the folding of longer DNA strands into hairpins, pseudoknots and cruciform.[123]
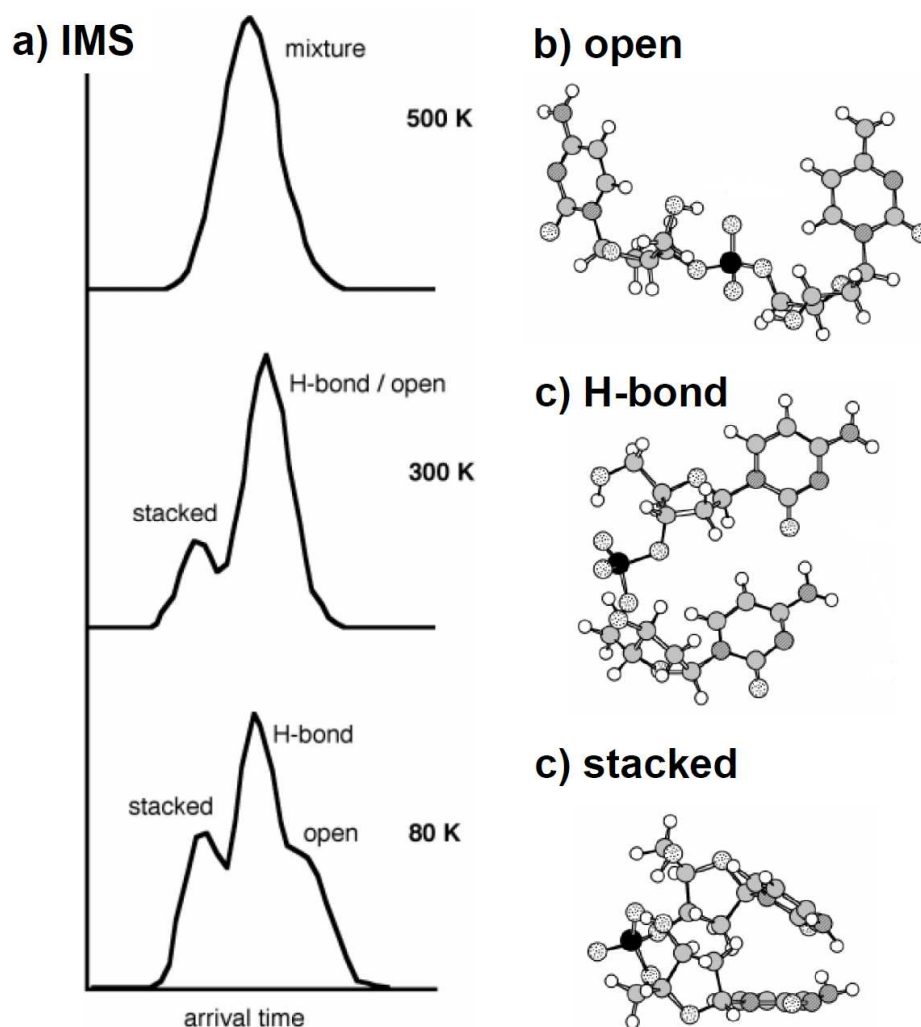
Figure 6: Structures of the dinucleotide dCC as a function of the temperature: (a) IMS experiments: arrival time distributions at three different temperatures. At 80K, three different structural families are distinguished. As the temperature increases, these structural families interconvert on the drift time scale (10^{-4} to 10^{-3} seconds). (b-d) Representative calculated structures for the three families. The H-bonded structure is the lowest in energy. (Figure adapted from Gidden et al., Eur. Phys. J. D, 2002,[121] with permission from Springer).

De Pauw's group used H/D exchange and ion mobility mass spectrometry as complementary techniques for the investigation of short oligonucleotides (DNAs dTG and dC_6, and RNA C_6).[58, 61] The drift cell of the IMS was used to perform the HDX reactions, when the exchange reagent is added to the buffer gas. Ion mobility experiments can thus provide information complementary to the HDX results. In the experiments conducted with different oligonucleotides, two situations were observed: for some oligonucleotides only a monomodal arrival-time distribution was obtained. This indicates that either only one structure exists or that

several conformers interconvert quickly on the time-scale of the experiment. In contrast, the C_6^{2-} oligomer appeared with two different structures in both experiments. Interestingly, they observed that the compact structure underwent a significantly faster exchange with the smallest CCS_{exp}.

The IMS-MS coupled to PES allows one to record the resolved photoelectron spectra after the separation of non-interconverting isomers by IMS and mass selection by MS. For each conformer separated according to overall compactness, the photoelectron spectra gives an indication on the charge locations. The coupling of IMS and PES was tested using the oligomer dC_6^{5-} as a test case,[105] and on $dN_x^{(x-1)-}$, x = 4, 5, and 6 oligonucleotides.[106] The results showed that for dC_4^{3-}, all dN_5^{4-}, and most dN_6^{5-} ions, a high-CCS conformation was characterized by a low electron binding energy contribution to photodetachment. This result is counterintuitive at first, because charge repulsion between the phosphates should give rise to both larger CCS and higher electron binding energy. The main conclusion is that, in highly charged oligonucleotides, conformers with all charges localized on the phosphates co-existed with conformers with at least one deprotonated terminal base. These protonation isomers did not interconvert on the ms time scale of the mobility separation, but proton movement from the base to the phosphate could be favoured by harsher source conditions. In conclusion, base deprotonation from multiply charged anions is possible (as also illustrated by a study of Monn and Schürch on methylphosphonate-modified oligonucleotides[124]), and proton transfer likely occurs in the gas phase.

V.2. Double Helix (duplex) DNA and duplex-drug complexes

The possibility to observe a DNA double helix in the gas phase was first demonstrated by Gale *et al.* who showed that by using an ESI-MS experiment, a dimer is detected intact.[125] So, even in the absence of water molecules and of counter-ions, and despite the multiple charges on the backbone of the DNA, the strands do not separate in the gas phase. It should be noted that depending on the state of charge of the duplex some phosphate units are charged, and some are deprotonated. The next question was whether these DNA dimers kept the B-form double helix that they had in solution. This questions was addressed theoretically[108], then experimentally[126].

The first extended MD was carried out on a microsecond scale to examine the changes in the DNA induced upon vaporization.[108] The authors found that vaporization of DNA, even at high temperatures, does not lead to a total separation or the disruption of the double helix. The transfer from solution phase to gas phase, produces some distortion of the helicity of the duplex but maintains the structural, energetic, and dynamic features of the conformation compared to the double helix in aqueous solution (Figure 7). The total number of DNA-DNA interactions is not dramatically different from that found in solution, and native interaction between bases was found

especially for the dinucleotide steps GpG . They also showed that even with different simulation protocol and definition of the model system, one can find that the gross geometric and energetic features of the DNA in the gas phase and in water to be very similar. However, one must be as close as experimental setups to be able to compare the structure in solution to the one in gas phase. In particular, compaction can be observed at higher temperature compared to room temperature.

The Bowers group studied the effect of the helicity in gas phase depending on the length of the oligomer by IMS and MD.[126, 127] A series of [poly d(CG)●poly d(CG)$_n$] duplexes were studied and observed that not only the duplexes are stable in the gas phase, but they can retain helical structures in solvent free environments. The results obtained showed that the increase in the length of the oligonucleotides ($\geq$ 10-mer) will increase the relative stability of the helicity and a helical structure is observed in IMS experiments. However for the 4-mer and 6-mer duplexes, only globular structures are observed. When the duplex reaches the 8-mer length, the globular form is the dominant conformer, but a small fraction of helical structures is also observed. Thus, the longer duplexes must have been helical in solution and retain that conformation for a limited time in the gas phase.[126] For AT-containing double-stranded DNA sequences, the ion mobility data reveal a more complex picture[128, 129], with fraying of AT regions when present at the extremities of the duplex, and bubble formation when present in the middle of the sequence.
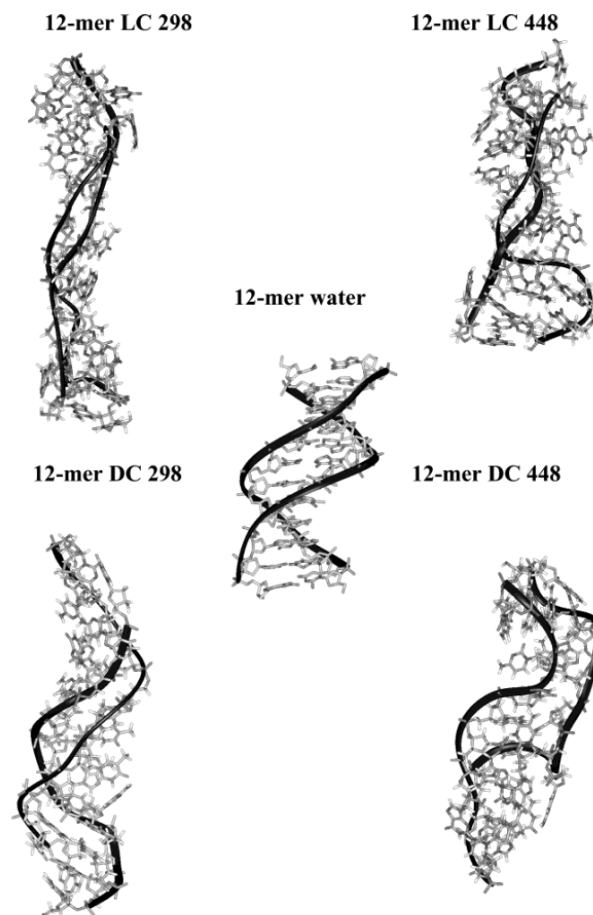
Figure 7: MD-averaged structures obtained for the 12-mer Dickerson-Drew self-complementary duplex (dCGCGAATTCGCG)$_2$, in water and in the gas phase at different temperatures (298K or 448K) and using different neutralization protocols (LC = localized charge, DC = delocalized charge). Averages were obtained in the 80-90 ns window. Reprinted with permission from Rueda et al., *J. Am. Chem. Soc.*, 2003, 125 (26), pp 8007–8014. Copyright 2003 American Chemical Society.

Structures in gas phase reflect the ones in the solution phase not only for duplex DNA alone. Early studies have indeed shown that even non covalent drug or ligands DNA complexes remain stable *in vacuo*.[117, 130] With MS, one can therefore establish in a single experiment the stoichiometry of the complexes and deduce relative affinities for a particular sequence quickly and easily and minimal sample consumption.[131] ESI-MS[132] and MS/MS[133, 134] was used for the study of the non-covalent binding of organic molecules (e.g. drugs) in the grooves of duplex DNAs. For groove binders, it was shown that the internal energy necessary to lead to strand separation depends on the ligand.[133] However, proton exchanges between the ligand and the DNA can lead to alternative dissociation pathways and can render the interpretation more difficult.[17] For neutral drugs, the collision energy required drug loss in gas phase MS/MS probing correlates well with

that in solution, suggesting that the ligand binding site remains the same in the gas phase as it was in solution.[17]

A MD study on the well-known minor groove binders was performed (DAPI, Hoechst 33258 and Netropsin) in the gas phase.[135] The authors show that by comparing simulation in water and in gas they could observe that the duplex is not dissociated and the complex conformer is not disrupted. However in the gas phase, they observe a large distortions in the double helix strands, but they suggest that they still maintain a memory of the original DNA structure. The minor groove binders are shown to remain bound to the DNA in a native preferential binding mode.

V.3. Triple Helix (triplex) DNA

The first DNA triplex structure was found stable in ESI-MS experiments under mild evaporation by Rosu *et al.*[136] In an ESI-FTICR-MS experiment in gas phase, the stability of four 14-mer triplexes were studied and compared to solution phase. The results showed that in the gas phase hydrogen bonds and electrostatic interactions predominate while in solution phase the stabilization of the triplex occurs through base stacking and hydrophobic interactions.[137] ESI-MS and ESI-MS/MS experiments coupled to MD also showed that one can study the interaction between triplex DNA and their ligand and to select ligands with better affinity and structural features towards the studied DNA molecule.[138]

On the theoretical side, an extensive MD simulation (more than 90 microseconds) was carried out to study the stability and the structures of the triplexes in gas phase, which were then validated by IMS-MS experiments.[139] Two stable parallel triplexes made of 12-mer and 18-mer were used. The results obtained show that the ensemble of structure of triplex is well-defined (Figure 8). However the degree of the distortion is as high as duplexes and less of what is observed of the G-quadruplexes. The good agreement between experimental and calculated CCS suggests that the structural models acquired adequately describe the triplexes produced by ESI-MS at their most abundant charge states. The data strongly supports that the gas phase triplex maintains an excellent memory of the solution structure, well-preserved helicity, and a significant number of native contacts, especially at low internal energies.[139] However, compaction of the structures is observed when the internal energy is increased (here, through the increase of the bias voltage before entering the IMS cell, see Figure 8c). The compaction of the structures depends highly on the state of charge: it is commonly observed that low charge state ions undergo compaction, and high charge state ions undergo expansion.[66, 140] For proteins, compaction is attributed to electrostatic interactions occurring via salt bridges or hydrogen bonds that stabilize

the molecule in the gas phase. [141] Linear structures are observed when the charge state is higher and Coulomb repulsions predominate.
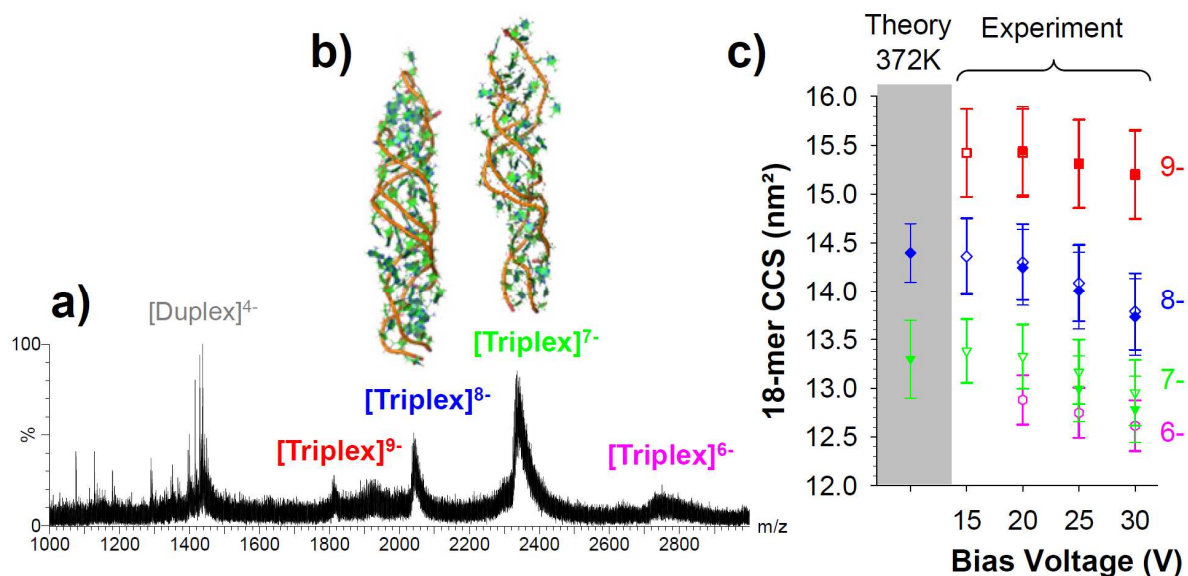

Figure 8: (a) ESI-MS spectra of the 18-mer triplex $d(TC^+)_9 \cdot d(GA)_9 \cdot d(TC)_9$ obtained from acidic conditions (150 mM NH_4OAc + acetic acid) at a bias voltage of 20 V on a Synapt HDMS ion mobility instrument. (b) Representative 3D structures obtained by MD in gas phase for the charge states 8- and 7-. (c) Agreement between theoretical and experimentally derived collision cross sections. Filled symbols: triplex with no ammonium adducts; open symbols: triplexes including the whole adduct distribution visible on the respective mass spectra. Adapted with permission from Arcella et al., J. Am. Chem. Soc., 2012, 134(15), pp 6596–6606. Copyright 2012 American Chemical Society.

V.4. G-Quadruplex DNA structures

Guanine-rich nucleic acids sequences are known to form higher order structures. G-quadruplexes are formed via a guanine tetrad, a square planar structure in which four guanines are associated through Hoogsteen hydrogen bonds (Figure 9a). These guanine tetrads stack on top of each other to form a G-quadruplex structure. Note that G-quadruplexes can be tetramolecular, bimolecular, or intramolecular. The tetrads are stabilized by the presence of cations in the middle of the planar square (Figure 9b). When transferred to the gas phase the structure of the G-quadruplexes is the most stable and keeps many native structural features. The quadruplexes were studied by ESI-MS and IMS and shown to be stable in gas phase as well, thanks to the conservation of the cations in-between the tetrads.[136, 142, 143] An extensive MD simulation of different types of G-quadruplexes stems (parallel and anti-parallel) showed in atomic details the

stability of the G-quadruplex stems and their ability to keep a memory of their solution structure in gas phase (Figure 9b).[144]

G-quadruplexes are to date the most stable model structure in gas phase since it does not go through severe distortion due to the stabilizing effect of the cations in the middle of the tetrads and the stacking between the guanine tetrads.[144] As a consequence, the measured CCS_{exp} of G-quadruplexes usually correlate well with the ones calculated assuming the preservation of the known solution-phase structure.[66, 128, 145] ESI-IMS experiments of G-quadruplexes with stabilizing ligands coupled to MD also showed a good representation of the structure in gas phase compared to the one in solution.[66] As a complementary approach to the IMS which gives information about the overall shape, ion spectroscopy was used to get structural information on the hydrogen bonding between the G-quartets (IRMPD ion spectroscopy) and on the base stacking (UV ion spectroscopy). The infrared signature (IRMPD) of G-quadruplexes in the gas phase revealed that H-bonding between guanines is preserved by following the carbonyl hydrogen stretching signals (Figure 9c).[93] UV spectroscopy of G-quadruplexes in gas phase gave also an indication about H bonding and base stacking and therefore giving a clear structure signature for the G-quadruplexes compared to the single strands (Figure 9d).[102] In summary, among all DNA higher-order structures studied to date, G-quadruplex DNA structures are most kinetically stable ones in the gas phase, provided that inter-quartet cations are conserved. They proved to be excellent model systems on which to test novel gas-phase structural probing methods.
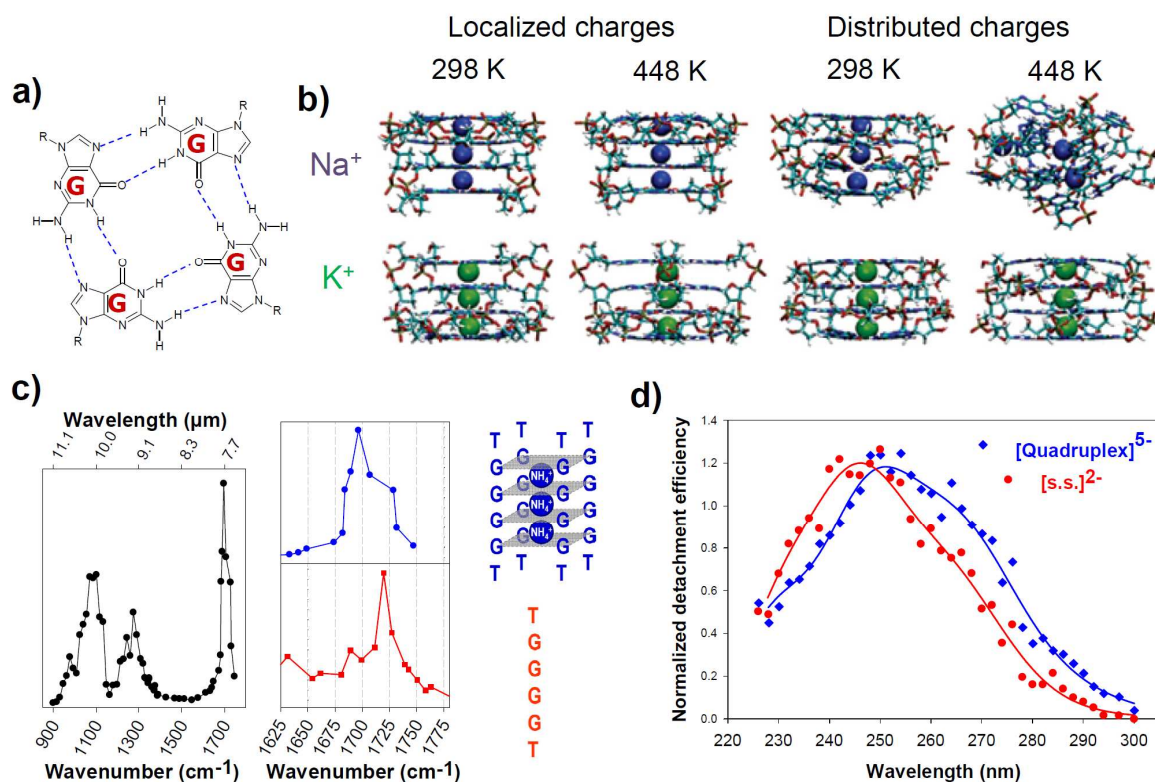
Figure 9: (a) Hydrogen bonding motif of a guanine quartet (G-quartet). (b) Final structures of 500-ns molecular dynamics in the gas phase for parallel-stranded $(dGGGG)_4^{5-}$, with trapped sodium or potassium. All trajectories are stable except with sodium at high temperature with the distributed charge model. Adapted with permission from Rueda et al., *J. Am. Chem. Soc.*, 2006, 128, 3608-3619. Copyright 2006 American Chemical Society. (c) Comparative IRMPD ion spectroscopy of single stranded[2-] (sequence shown in red) and G-quadruplex[5-] (structure shown in blue with the intercalation of 3 ammonium anions between the G quartets) forms of dTGGGGT. Left: full IRMPD spectrum of the G-quadruplex in the gas phase. Right: the carbonyl band shifts to the red upon G-quadruplex formation, due to hydrogen bonding. Adapted with permission from Gabelica et al., *J. Am. Chem. Soc.*, 2008, 130, 1810-1811. Copyright 2008 American Chemical Society. (d) Comparative UV action spectra of the same single strand and G-quadruplex. UV absorption shifts to the red in the G-quadruplex, presumably due to G-quartet stacking. Adapted with permission from Rosu et al., *J. Phys. Chem. A*, 2012, 116, 5383–5391. Copyright 2012 American Chemical Society.

V.5. RNA structures in the gas phase

RNA structures have been more extensively studied than DNA ones by in-solution probing monitored by MS (see Section III.1 above). However, there are much fewer studies on direct probing of RNA structures in gas phase as compared to DNA. MS/MS where fragmentation was

caused by collision-induced dissociation (CID) or single-wavelength IRMPD were the most widely used to date, for structural probing and to determine the tertiary structure of the RNA folding and to define the single stranded loops, the pseudo knot from the intact double stranded.[47] Apart from the IMS and HDX study on the hexamer RNA C_6 that was described above[58], no detailed IMS or theoretical simulation in the gas phase to characterize RNA atomic detailed structure was reported to date.

VI. Conclusions and perspectives

VI.1. Particularities of nucleic acid structures in the gas phase

A fundamental question in native mass spectrometry is the extent to which non-covalent interactions, responsible for subunit folding and inter-subunit interactions, are conserved when a complex is transferred from the solution to the gas phase. While this question is identical for all systems, from biomolecules (proteins, nucleic acids, carbohydrates,…) to synthetic supramolecular complexes, the specific answers will vary depending on the types of interactions (salt bridges, hydrogen bonding, van der Waals, hydrophobic,…) prevailing in the system of interest. Compared to proteins, nucleic acids present a more rugged free energy landscape in solution, owing to the numerous hydrogen bonds and ionic interactions involved in their native functional structures. In the gas phase, these types of interactions are further reinforced. For multiply charged anions, the kinetic stability of nucleic acid structures ranks as follows: duplex (hydrogen bonding interactions) < triplex and *i*-motif (proton-mediated hydrogen bonding) < G-quadruplex (cation coordination and hydrogen bonding). Zwitterion formation and cation coordination helps keeping some ionic interactions in place, and help avoiding rearrangements due to self-solvation. The gas phase environment shows clearly an enthalpy/entropy compensation effect. Indeed, molecular dynamics trajectories indicate that the conformational entropy of isolated structures in the gas phase is low for G-quadruplexes (which are very rigid thanks to their inner cations), and increases for triplexes, i-motifs, duplexes and single strands while enthalpy-favourable interactions decrease.

The effect of cation coordination on other gas-phase nucleic acid structures than G-quadruplexes, therefore seems extremely worthy of further investigation. In particular, RNA tridimensional structures have not been investigated by direct probing in the gas phase, and there are numerous questions we need to answer: Are hairpins conserved in the gas phase? Is there a

minimum stem length or stability to ensure conservation? Is the coaxial stacking of helices preserved in the gas phase? Are specifically cations like Mg^{2+} needed to preserve some structures? How does the conservation of each motif depend on the ion effective temperature, the ion charge state and time spent in the gas phase?

VI.2. Opportunities and challenges in gas-phase structural biology of nucleic acids

The rugged free energy landscape in solution presents specific challenges for standard structural biology, and not all nucleic acids are amenable to NMR or X-ray crystallography. Several folding pathways often coexist, and some metastable states can be very long-lived (seconds or longer). Besides, ligand-mediated regulation is sometimes under kinetic control. Metastable states can therefore be as important functionally as the thermodynamically most stable state. Experimental techniques to characterize all co-existing states in the conformational ensemble, including minor ones, are therefore crucial.

By bringing each structure or each complex co-existing in solution to the gas phase, gas-phase structural probing methods have the potential to find applications in many areas of nucleic acid studies. Moreover, in the future, the study of biomolecule structures in gas phase have the potential to become resolved with atomistic detail, especially with the recent development of the X-ray free-electron laser (X-FEL) diffraction.[146] As well, the Ultrafast electron diffraction (UED) showed the first successful electron diffraction of biomolecules achieved with surface-assisted infrared laser desorption by determining the structures of the RNA nucleobase, uracil, and the DNA nucleobase, guanine. [147] In a less distant future, different approaches currently mainly developed either for proteins, or for smaller nucleic acid building blocks, will likely be applied to study nucleic acid oligonucleotides and tridimensional structures thereof. The key is to combine several approach, either in parallel or in a hyphenated manner (i.e., on a single instrument). For example, the combination of conformation information (IMS) and local information (electron or ion spectroscopy) should be more extensively developed and would give a more detailed view of the studied system, as shown by a few leading papers.[98, 105, 106]

Closely related to electronic ion spectroscopy is the need for better understanding the nature and fate of electronic excited states of DNA/RNA bases, isolated and in the context of higher-order structures. Stacking is particularly challenging to deal with, but of prime importance both on the structural, analytical, and on the photostability point of views. De Vries *et al.* had pioneered this research for nucleobases.[95-97] The development of UV, VUV (vacuum ultraviolet, i.e., 5-20 eV),[148-150] and high-energy ion beam collision setups[151, 152] will be important for further fundamental investigation of DNA photostability.

In the field of DNA G-quadruplexes, which are the best preserved in the gas phase, mass spectrometry is more and more routinely combined with in-solution structural and biophysics techniques to study NA folding or ligand binding.[153-158] This kind of application to solution phase problems however requires that the key structural elements are preserved or modified in a predictable way such that the gas phase structure keeps a memory of the initial structure in solution. A task lying ahead is to determine the range of other NA structures for which preservation is most likely, and in which conditions.

Another challenge is to make advances in both experimental and theoretical methodologies tailor-made for nucleic acids. Ion mobility spectrometry is a low resolution experiment which showed its high potential for probing NAs structures and determining global shape. It is therefore sensitive to tertiary structures of large assemblies, and to secondary structures for smaller ones consisting of a single major motif. With this advance in MS, advances also were made in the theoretical approaches to support the experimental collision cross sections with calculated ones. Challenges however remain to bridge the gap between theory and experiments, with regard to temperature and time scale definition, charge localization etc.... MD simulations to date on various forms of DNA showed that the overall structure and feature of the molecules in gas-phase are well maintained. However, MD simulations predict distortions in the helix parameters. Ion spectroscopy techniques have the potential to provide complementary information on the gas-phase structures. Vibrational (IRMPD) spectroscopy is the more advanced to date, but remains generally applicable to small systems only. Electronic spectroscopy in the gas phase is still in its infancy. However, by analogy with the solution-phase studies, electronic circular dichroism[4, 159] and fluorescence lifetime spectroscopy[160, 161] would be extremely useful to probe stacking interactions. Transposing these ion spectroscopy approaches to the gas phase would constitute major advances in the field.

References

1.   B. H. Mooers, *Methods*, 2009, **47**, 168-176.
2.   Z. Shajani and G. Varani, *Biopolymers*, 2007, **86**, 348-359.
3.   L. Zidek, R. Stefl and V. Sklenar, *Curr Opin Struct Biol*, 2001, **11**, 275-281.
4.   J. Kypr, I. Kejnovska, D. Renciuk and M. Vorlickova, *Nucleic Acids Res*, 2009, **37**, 1713-1725.
5.   J. Lipfert and S. Doniach, *Annu Rev Biophys Biomol Struct*, 2007, **36**, 307-327.
6.   R. Beveridge, Q. Chappuis, C. Macphee and P. Barran, *The Analyst*, 2013, **138**, 32-42.
7.   A. A. Rostom, P. Fucini, D. R. Benjamin, R. Juenemann, K. H. Nierhaus, F. U. Hartl, C. M. Dobson and C. V. Robinson, *Proc Natl Acad Sci U S A*, 2000, **97**, 5185-5190.
8.   S. D. Fuerstenau and W. H. Benner, *Rapid Commun Mass Spectrom*, 1995, **9**, 1528-1538.
9.   R. Chen, X. Cheng, D. W. Mitchell, S. A. Hofstadler, Q. Wu, A. L. Rockwood, M. G. Sherman and R. D. Smith, *Anal Chem*, 1995, **67**, 1159-1163.
10.   B. Heddi, N. Foloppe, E. Hantz and B. Hartmann, *J Mol Biol*, 2007, **368**, 1403-1411.
11.   T. Meyer, V. Gabelica, H. Grubmüller and M. Orozco, *WIREs Comput Mol Sci*, 2013, **3**, 408-425.
12.   J. L. Benesch and C. V. Robinson, *Nature*, 2009, **462**, 576-577.
13.   S. Yin and J. A. Loo, *Int J Mass Spectrom*, 2011, **300**, 118-122.
14.   A. Y. Park and C. V. Robinson, *Crit Rev Biochem Mol Biol*, 2011, **46**, 152-164.
15.   V. Gabelica, *Nucleic Acids in the Gas Phase*, Springer-Verlag, Berlin Heidelberg, 2014.
16.   J. B. Fenn, M. Mann, C. K. Meng, S. F. Wong and C. M. Whitehouse, *Science*, 1989, **246**, 64-71.
17.   F. Rosu, S. Pirotte, E. D. Pauw and V. Gabelica, *Int. J. Mass Spectrom.*, 2006, **253**, 156-171.
18.   K. A. Sannes-Lowery, D. P. Mack, P. Hu, H.-Y. Mei and J. A. Loo, *J Am Soc Mass Spectrom*, 1997, **8**, 90-95.
19.   H. Saigusa, *J Photoch Photobio C*, 2006, **7**, 197-210.
20.   S. J. Gaskell, *J Mass Spectrom*, 1997, **32**, 677-688.
21.   J. B. Fenn, *J Am Soc Mass Spectrom*, 1993, **4**, 524-535.
22.   M. Hautreux, N. Hue, A. Du Fou de Kerdaniel, A. Zahir, V. Malec and O. Laprévote, *Int. J. Mass Spectrom.*, 2004, **231**, 131-137.
23.   L. Konermann, E. Ahadi, A. D. Rodriguez and S. Vahidi, *Anal Chem*, 2013, **85**, 2-9.
24.   K. Vékey, *J Mass Spectrom*, 1996, **31**, 445-463.
25.   V. Gabelica and E. De Pauw, *Mass Spectrom Rev*, 2005, **24**, 566-587.
26.   M. Z. Steinberg, K. Breuker, R. Elber and R. B. Gerber, *Phys Chem Chem Phys*, 2007, **9**, 4690-4697.
27.   M. Z. Steinberg, R. Elber, F. W. McLafferty, R. B. Gerber and K. Breuker, *Chembiochem*, 2008, **9**, 2417-2423.
28.   S. C. Gibson, C. S. Feigerle and K. D. Cook, *Anal Chem*, 2014, **86**, 464-472.
29.   P. A. Limbach, P. F. Crain and J. A. McCloskey, *Nucleic Acids Res*, 1994, **22**, 2183-2196.
30.   W. A. Cantara, P. F. Crain, J. Rozenski, J. A. McCloskey, K. A. Harris, X. Zhang, F. A. Vendeix, D. Fabris and P. F. Agris, *Nucleic Acids Res*, 2011, **39**, D195-201.
31.   M. P. Stone, H. Huang, K. L. Brown and G. Shanmugam, *Chem Biodivers*, 2011, **8**, 1571-1615.
32.   D. Fabris and E. T. Yu, *J Mass Spectrom*, 2010, **45**, 841-860.
33.   E. T. Yu, Q. Zhang and D. Fabris, *J Mol Biol*, 2005, **345**, 69-80.
34.   J. Yang, J. J. Mo, J. T. Adamson and K. Hakansson, *Analytical Chemistry*, 2005, **77**, 1876-1882.
35.   Y. Gao, J. Yang, M. T. Cancilla, F. Meng and S. A. McLuckey, *Anal Chem*, 2013, **85**, 4713-4720.
36.   V. Gabelica, T. Tabarin, R. Antoine, F. Rosu, I. Compagnon, M. Broyer, E. De Pauw and P. Dugourd, *Anal Chem*, 2006, **78**, 6564-6572.
37.   M. T. Krahmer, J. J. Walters, K. F. Fox, A. Fox, K. E. Creek, L. Pirisi, D. S. Wunschel, R. D. Smith, D. L. Tabb and J. R. Yates, 3rd, *Anal Chem*, 2000, **72**, 4033-4040.
38.   S. Schurch, J. M. Tromp and S. T. Monn, *Nucleos nucleot nucl*, 2007, **26**, 1629-1633.
39.   S. T. Monn and S. Schurch, *J Am Soc Mass Spectrom*, 2007, **18**, 984-990.
40.   S. A. McLuckey and S. Habibi-Goudarzi, *J Am Soc Mass Spectrom*, 1994, **5**, 740-747.
41.   S. I. Smith and J. S. Brodbelt, *Anal Chem*, 2011, **83**, 303-310.
42.   R. G. Brinson, K. B. Turner, H. Y. Yi-Brunozzi, S. F. Le Grice, D. Fabris and J. P. Marino, *Biochemistry*, 2009, **48**, 6988-6997.

43. K. B. Turner, A. S. Kohlway, N. A. Hagan and D. Fabris, *Biopolymers*, 2009, **91**, 283-296.
44. K. B. Turner, R. G. Brinson, H. Y. Yi-Brunozzi, J. W. Rausch, J. T. Miller, S. F. Le Grice, J. P. Marino and D. Fabris, *Nucleic Acids Res*, 2008, **36**, 2799-2810.
45. K. B. Turner, N. A. Hagan, A. S. Kohlway and D. Fabris, *J Am Soc Mass Spectrom*, 2006, **17**, 1401-1411.
46. S. A. McLuckey, *J Am Soc Mass Spectrom*, 1992, **3**, 599-614.
47. D. Fabris, K. A. Kellersberger and J. A. Wilhide, *Int J Mass Spectrom*, 2012, **312**, 155-162.
48. J. Mo and K. Hakansson, *Anal Bioanal Chem*, 2006, **386**, 675-681.
49. P. D. Schnier, J. S. Klassen, E. F. Strittmatter and E. R. Williams, *J Am Chem Soc*, 1998, **120**, 9605-9613.
50. V. Gabelica and E. De Pauw, *Int. J. Mass Spectrom.*, 2002, **219**, 151-159.
51. R. C. Dunbar, *Mass Spectrom Rev*, 2004, **23**, 127-158.
52. J. S. Klassen, P. D. Schnier and E. R. Williams, *J Am Soc Mass Spectrom*, 1998, **9**, 1117-1124.
53. R. Daneshfar and J. S. Klassen, *J Am Soc Mass Spectrom*, 2006, **17**, 1229-1238.
54. R. Daneshfar and J. S. Klassen, *J Am Soc Mass Spectrom*, 2004, **15**, 55-64.
55. M. Schäfer, C. Schmuck, M. Heil, H. J. Cooper, C. L. Hendrickson, M. J. Chalmers and A. G. Marshall, *Journal of the American Society for Mass Spectrometry*, 2003, **14**, 1282-1289.
56. T. Doussineau, R. Antoine, M. Santacreu and P. Dugourd, *J Phys Chem Lett*, 2012, **3**, 2141-2145.
57. R. Antoine, T. Doussineau, P. Dugourd and F. Calvo, *Phys Rev A*, 2013, **87**, 013435.
58. D. Balbeur, J. Widart, B. Leyh, L. Cravello and E. De Pauw, *J Am Soc Mass Spectrom*, 2008, **19**, 938-946.
59. K. D. Rand, S. D. Pringle, M. Morris and J. M. Brown, *Anal Chem*, 2012, **84**, 1931-1940.
60. J. Mo, G. C. Todd and K. Hakansson, *Biopolymers*, 2009, **91**, 256-264.
61. D. Balbeur, D. Dehareng and E. De Pauw, *J Am Soc Mass Spectrom*, 2007, **18**, 1827-1834.
62. J. E. Chipuk and J. S. Brodbelt, *Int J Mass Spectrom*, 2009, **287**, 87-95.
63. V. Gabelica, F. Rosu, M. Witt, G. Baykut and E. De Pauw, *Rapid Commun Mass Spectrom*, 2005, **19**, 201-208.
64. C. Lapthorn, F. Pullen and B. Z. Chowdhry, *Mass Spectrom Rev*, 2013, **32**, 43-71.
65. F. Lanucara, S. W. Holman, C. J. Gray and C. E. Eyers, *Nat Chem*, 2014, **6**, 281-294.
66. V. Gabelica, E. S. Baker, M. P. Teulade-Fichou, E. De Pauw and M. T. Bowers, *J Am Chem Soc*, 2007, **129**, 895-904.
67. T. Wyttenbach, G. Helden, J. Batka, D. Carlat and M. Bowers, *J Am Soc Mass Spectrom*, 1997, **8**, 275-282.
68. A. A. Shvartsburg and M. F. Jarrold, *Chem Phys Lett*, 1996, **261**, 86-91.
69. A. A. Shvartsburg, G. C. Schatz and M. F. Jarrold, *J Chem Phys*, 1998, **108**, 2416-2423.
70. A. A. Shvartsburg, S. V. Mashkevich, E. S. Baker and R. D. Smith, *J Phys Chem A*, 2007, **111**, 2002-2010.
71. C. K. Siu, Y. Guo, I. S. Saminathan, A. C. Hopkinson and K. W. Siu, *J Phys Chem B*, 2010, **114**, 1204-1212.
72. C. Bleiholder, S. Contreras, T. D. Do and M. T. Bowers, *Int. J. Mass Spectrom.*, 2013, **345–347**, 89-96.
73. C. Wiley Interdisciplinary Reviews: Computational Molecular ScienceBleiholder, T. Wyttenbach and M. T. Bowers, *Int. J. Mass Spectrom.*, 2011, **308**, 1-10.
74. T. Wyttenbach, C. Bleiholder and M. T. Bowers, *Anal Chem*, 2013, **85**, 2191-2199.
75. C. Bleiholder, S. Contreras and M. T. Bowers, *Int J Mass Spectrom*, 2013, **354–355**, 275-280.
76. C. Larriba and C. J. Hogan, Jr., *J Phys Chem A*, 2013, **117**, 3887-3901.
77. J. C. May, C. R. Goodwin, N. M. Lareau, K. L. Leaptrot, C. B. Morris, R. T. Kurulugama, A. Mordehai, C. Klein, W. Barry, E. Darland, G. Overney, K. Imatani, G. C. Stafford, J. C. Fjeldsted and J. A. McLean, *Anal Chem*, 2014, **86**, 2107-2116.
78. J. L. Alonso, I. Pena, J. C. Lopez and V. Vaquero, *Angew Chem Int Ed Engl*, 2009, **48**, 6141-6143.

79.   J. L. Alonso, V. Vaquero, I. Pena, J. C. Lopez, S. Mata and W. Caminati, *Angew Chem Int Ed Engl*, 2013, **52**, 2331-2334.
80.   V. Vaquero, M. E. Sanz, J. C. Lopez and J. L. Alonso, *J Phys Chem A*, 2007, **111**, 3443-3445.
81.   A. L. Steber, J. L. Neill, D. P. Zaleski, B. H. Pate, A. Lesarri, R. G. Bird, V. Vaquero-Vara and D. W. Pratt, *Faraday Discuss*, 2011, **150**, 227-242; discussion 257-292.
82.   J. C. Lopez, M. I. Pena, M. E. Sanz and J. L. Alonso, *J Chem Phys*, 2007, **126**, 191103.
83.   J. Y. Salpin, S. Guillaumont, J. Tortajada, L. MacAleese, J. Lemaire and P. Maitre, *Chemphyschem*, 2007, **8**, 2235-2244.
84.   M. B. Burt and T. D. Fridgen, *Eur J Mass Spectrom (Chichester, Eng)*, 2012, **18**, 235-250.
85.   J. M. Bakker, J.-Y. Salpin and P. Maître, *Int. J. Mass Spectrom.*, 2009, **283**, 214-221.
86.   J. M. Bakker, R. K. Sinha, T. Besson, M. Brugnara, P. Tosi, J. Y. Salpin and P. Maitre, *J Phys Chem A*, 2008, **112**, 12393-12400.
87.   S. O. Pedersen, C. S. Byskov, F. Turecek and S. B. Nielsen, *J Phys Chem A*, 2014, **118**, 4256-4265.
88.   G. Féraud, C. Dedonder, C. Jouvet, Y. Inokuchi, T. Haino, R. Sekiya and T. Ebata, *J Phys Chem Lett*, 2014, **5**, 1236-1240.
89.   M. Berdakin, G. Feraud, C. Dedonder-Lardeux, C. Jouvet and G. A. Pino, *Physical chemistry chemical physics : PCCP*, 2014, **16**, 10643-10650.
90.   B. Yang, R. R. Wu, G. Berden, J. Oomens and M. T. Rodgers, *J Phys Chem B*, 2013, **117**, 14191-14201.
91.   Y. W. Nei, K. T. Crampton, G. Berden, J. Oomens and M. T. Rodgers, *J Phys Chem A*, 2013, **117**, 10634-10649.
92.   Y. W. Nei, N. Hallowita, J. D. Steill, J. Oomens and M. T. Rodgers, *J Phys Chem A*, 2013, **117**, 1319-1335.
93.   V. Gabelica, F. Rosu, E. De Pauw, J. Lemaire, J. C. Gillet, J. C. Poully, F. Lecomte, G. Gregoire, J. P. Schermann and C. Desfrancois, *J Am Chem Soc*, 2008, **130**, 1810-1811.
94.   F. Rosu, V. Gabelica, L. Joly, G. Gregoire and E. De Pauw, *Phys Chem Chem Phys*, 2010, **12**, 13448-13454.
95.   K. Kleinermanns, D. Nachtigallová and M. S. de Vries, *Int rev Phys Chem*, 2013, **32**, 308-342.
96.   E. Nir, K. Kleinermanns and M. S. de Vries, *Nature*, 2000, **408**, 949-951.
97.   C. Plutzer, I. Hunig, K. Kleinermanns, E. Nir and M. S. de Vries, *Chemphyschem*, 2003, **4**, 838-842.
98.   G. Papadopoulos, A. Svendsen, O. V. Boyarkin and T. R. Rizzo, *Faraday Discuss*, 2011, **150**, 243-255; discussion 257-292.
99.   G. Papadopoulos, A. Svendsen, O. V. Boyarkin and T. R. Rizzo, *J Am Soc Mass Spectrom*, 2012, **23**, 1173-1181.
100.   L. M. Nielsen, S. O. Pedersen, M. B. Kirketerp and S. B. Nielsen, *J Chem Phys*, 2012, **136**, 064302.
101.   S. O. Pedersen, K. Stochkel, C. S. Byskov, L. M. Baggesen and S. B. Nielsen, *Phys Chem Chem Phys*, 2013, **15**, 19748-19752.
102.   F. Rosu, V. Gabelica, E. De Pauw, R. Antoine, M. Broyer and P. Dugourd, *J Phys Chem A*, 2012, **116**, 5383-5391.
103.   A. S. Danell and J. H. Parks, *J Am Soc Mass Spectrom*, 2003, **14**, 1330-1339.
104.   J. M. Weber, I. N. Ioffe, K. M. Berndt, D. Loffler, J. Friedrich, O. T. Ehrler, A. S. Danell, J. H. Parks and M. M. Kappes, *J Am Chem Soc*, 2004, **126**, 8585-8589.
105.   M. Vonderach, O. T. Ehrler, P. Weis and M. M. Kappes, *Anal Chem*, 2011, **83**, 1108-1115.
106.   M. Vonderach, O. T. Ehrler, K. Matheis, P. Weis and M. M. Kappes, *J Am Chem Soc*, 2012, **134**, 7830-7841.
107.   C. S. Hoaglund, Y. Liu, A. D. Ellington, M. Pagel and D. E. Clemmer, *J Am Chem Soc*, 1997, **119**, 9051-9052.
108.   M. Rueda, S. G. Kalko, F. J. Luque and M. Orozco, *J Am Chem Soc*, 2003, **125**, 8007-8014.
109.   J. Gidden and M. T. Bowers, *J Phys Chem B*, 2003, **107**, 12829-12837.
110.   X. Yang, X. B. Wang, E. R. Vorpagel and L. S. Wang, *Proc Natl Acad Sci U S A*, 2004, **101**, 17588-17592.

111. V. V. Zakjevskii, S. J. King, O. Dolgounitcheva, V. G. Zakrzewski and J. V. Ortiz, *J Am Chem Soc*, 2006, **128**, 13350-13351.
112. A. Abo-riziq, B. O. Crews, I. Compagnon, J. Oomens, G. Meijer, G. Von Helden, M. Kabelac, P. Hobza and M. S. de Vries, *J Phys Chem A*, 2007, **111**, 7529-7536.
113. N. Leulliot, M. Ghomi, H. Jobic, O. Bouloussa, V. Baumruk and C. Coulombeau, *J Phys Chem B*, 1999, **103**, 10934-10944.
114. N. Leulliot, M. Ghomi, G. Scalmani and G. Berthier, *J Phys Chem A*, 1999, **103**, 8716-8724.
115. B. Chiavarino, M. E. Crestoni, S. Fornarini, F. Lanucara, J. Lemaire, P. Maitre and D. Scuderi, *Int. J. Mass Spectrom.*, 2008, **270**, 111-117.
116. M. K. Shukla and J. Leszczynski, *J Comput Chem*, 2004, **25**, 768-778.
117. R. Improta, *Chemistry*, 2014, **20**, 8106-8115.
118. A. Perez, I. Marchan, D. Svozil, J. Sponer, T. E. Cheatham, 3rd, C. A. Laughton and M. Orozco, *Biophys J*, 2007, **92**, 3817-3829.
119. K. Breuker and F. W. McLafferty, *Proc Natl Acad Sci U S A*, 2008, **105**, 18145-18152.
120. T. Meyer, X. de la Cruz and M. Orozco, *Structure*, 2009, **17**, 88-95.
121. J. Gidden and M. T. Bowers, *Eur. Phys. J. D*, 2002, **20**, 409-419.
122. J. Gidden and M. T. Bowers, *J Am Soc Mass Spectrom*, 2003, **14**, 161-170.
123. E. S. Baker, N. F. Dupuis and M. T. Bowers, *J Phys Chem B*, 2009, **113**, 1722-1727.
124. C. Truillet, F. Lux, O. Tillement, P. Dugourd and R. Antoine, *Anal Chem*, 2013, **85**, 10440-10447.
125. D. C. Gale and R. D. Smith, *J Am Soc Mass Spectrom*, 1995, **6**, 1154-1164.
126. J. Gidden, A. Ferzoco, E. S. Baker and M. T. Bowers, *J Am Chem Soc*, 2004, **126**, 15132-15140.
127. E. S. Baker and M. T. Bowers, *J Am Soc Mass Spectrom*, 2007, **18**, 1188-1195.
128. J. Gidden, E. S. Baker, A. Ferzoco and M. T. Bowers, *International Journal of Mass Spectrometry*, 2005, **240**, 183-193.
129. A. Burmistrova, V. Gabelica, A. S. Duwez and E. De Pauw, *J Am Soc Mass Spectrom*, 2013, **24**, 1777-1786.
130. S. A. Hofstadler and R. H. Griffey, *Chem Rev*, 2001, **101**, 377-390.
131. F. Rosu, E. De Pauw and V. Gabelica, *Biochimie*, 2008, **90**, 1074-1087.
132. K. X. Wan, T. Shibue and M. L. Gross, *J Am Chem Soc*, 1999, **122**, 300-307.
133. V. Gabelica, F. Rosu, C. Houssier and E. De Pauw, *Rapid Commun Mass Spectrom*, 2000, **14**, 464-467.
134. K. X. Wan, M. L. Gross and T. Shibue, *J Am Soc Mass Spectrom*, 2000, **11**, 450-457.
135. M. Rueda, F. J. Luque and M. Orozco, *J Am Chem Soc*, 2005, **127**, 11690-11698.
136. F. Rosu, V. Gabelica, C. Houssier, P. Colson and E. D. Pauw, *Rapid Commun Mass Spectrom*, 2002, **16**, 1729-1736.
137. C. Wan, X. Guo, Z. Liu and S. Liu, *J Mass Spectrom*, 2008, **43**, 164-172.
138. F. Rosu, C. H. Nguyen, E. De Pauw and V. Gabelica, *J Am Soc Mass Spectrom*, 2007, **18**, 1052-1062.
139. A. Arcella, G. Portella, M. L. Ruiz, R. Eritja, M. Vilaseca, V. Gabelica and M. Orozco, *J Am Chem Soc*, 2012, **134**, 6596-6606.
140. F. Balthasart, J. Plavec and V. Gabelica, *J. Am. Soc. Mass Spectrom.*, 2013, **24**, 1-8.
141. M. Schennach and K. Breuker, *Angew Chem Int Ed Engl*, 2014, **53**, 164-168.
142. M. Vairamani and M. L. Gross, *J Am Chem Soc*, 2003, **125**, 42-43.
143. F. Balthasart, J. Plavec and V. Gabelica, *J Am Soc Mass Spectrom*, 2013, **24**, 1-8.
144. M. Rueda, F. J. Luque and M. Orozco, *J Am Chem Soc*, 2006, **128**, 3608-3619.
145. E. S. Radiation Physics and ChemistryBaker, S. L. Bernstein, V. Gabelica, E. De Pauw and M. T. Bowers, *Int J Mass Spectrom*, 2006, **253**, 225-237.
146. R. Neutze, G. Huldt, J. Hajdu and D. van der Spoel, *Rad Phys Chem*, 2004, **71**, 905-916.
147. A. Gahlmann, S. T. Park and A. H. Zewail, *J Am Chem Soc*, 2009, **131**, 2806-2808.
148. E. Dupre, A. Wohlkonig, J. Herrou, C. Locht, F. Jacob-Dubuisson and R. Antoine, *BMC microbiology*, 2013, **13**, 172.

149. Q. Enjalbert, C. Brunet, A. Vernier, A. R. Allouche, R. Antoine, P. Dugourd, J. Lemoine, A. Giuliani and L. Nahon, *J Am Soc Mass Spectrom*, 2013, **24**, 1271-1279.
150. J. Morlieras, S. Dufort, L. Sancey, C. Truillet, A. Mignot, F. Rossetti, M. Dentamaro, S. Laurent, L. Vander Elst, R. N. Muller, R. Antoine, P. Dugourd, S. Roux, P. Perriat, F. Lux, J. L. Coll and O. Tillement, *Bioconjugate chemistry*, 2013, **24**, 1584-1597.
151. C. Brunet, R. Antoine, P. Dugourd, F. Canon, A. Giuliani and L. Nahon, *J Chem Phys*, 2013, **138**, 064301.
152. S. Martin, C. Ortega, L. Chen, R. Brédy, A. Vernier, P. Dugourd, R. Antoine, J. Bernard, G. Reitsma, O. Gonzalez-Magaña, R. Hoekstra and T. Schlathölter, *Phys Rev A*, 2014, **89**, 012707.
153. J. Zhou, A. Bourdoncle, F. Rosu, V. Gabelica and J. L. Mergny, *Angew Chem Int Ed Engl*, 2012, **51**, 11002-11005.
154. N. M. Smith, S. Amrane, F. Rosu, V. Gabelica and J. L. Mergny, *Chem Commun (Camb)*, 2012, **48**, 11464-11466.
155. L. Joly, F. Rosu and V. Gabelica, *Chem Commun (Camb)*, 2012, **48**, 8386-8388.
156. N. Borbone, J. Amato, G. Oliviero, V. D'Atri, V. Gabelica, E. De Pauw, G. Piccialli and L. Mayol, *Nucleic Acids Res*, 2011, **39**, 7848-7857.
157. F. Rosu, V. Gabelica, H. Poncelet and E. De Pauw, *Nucleic Acids Res*, 2010, **38**, 5217-5225.
158. S. E. Pierce, J. Wang, J. Jayawickramarajah, A. D. Hamilton and J. S. Brodbelt, *Chemistry*, 2009, **15**, 11244-11255.
159. A. I. Holm, L. M. Nielsen, S. V. Hoffmann and S. B. Nielsen, *Phys Chem Chem Phys*, 2010, **12**, 9581-9596.
160. I. Vaya, T. Gustavsson, F. A. Miannay, T. Douki and D. Markovitsi, *J Am Chem Soc*, 2010, **132**, 11834-11835.
161. C. T. Middleton, K. de La Harpe, C. Su, Y. K. Law, C. E. Crespo-Hernández and B. Kohler, *Annu Rev Phys Chem*, 2009, **60**, 217-239.